U.S. Department
of Transportation
National Highway
Traffic Safety
Administration

NHTSA

DOT HS 813 540b

May 2024

Restraint Design for Obese Occupants: Rear-Seat Simulations

Page intentionally left blank.

DISCLAIMER

This publication is distributed by the U.S. Department of Transportation, National Highway Traffic Safety Administration, in the interest of information exchange. The opinions, findings, and conclusions expressed in this publication are those of the authors and not necessarily those of the Department of Transportation or the National Highway Traffic Safety Administration. The United States Government assumes no liability for its contents or use thereof. If trade or manufacturers' names or products are mentioned, it is because they are considered essential to the object of the publication and should not be construed as an endorsement. The United States Government does not endorse products or manufacturers.

NOTE: This report is published in the interest of advancing motor vehicle safety research. While the report may provide results from research or tests using specifically identified motor vehicle models, it is not intended to make conclusions about the safety performance or safety compliance of those motor vehicles, and no such conclusions should be drawn.

Suggested APA Format Citation:

Kerrigan, J. R., Joodaki, H., Sun, Z., & Gepner, B. (2024, May). *Restraint design for obese occupants: Rear-seat simulations* (Second of four parts. Report No. DOT HS 813 540b). National Highway Traffic Safety Administration.

The other three parts of this series:

Joodaki, H., Gepner, B., & Kerrigan, J. R. (2024, May). *Restraint design for obese occupants* (First of four parts. Report No. DOT HS 813 540a). National Highway Traffic Safety Administration.

Sun, Z., Kerrigan, J. R., Joodaki, H., and & Gepner, B. (2024, May). *Restraint design for obese occupants: Belt pull test simulations error effects modeling* (Third of four parts. Report No. DOT HS 813 540c). National Highway Traffic Safety Administration.

Kerrigan, J. R., Forman, J., Gepner, B., Joodaki, H., & Sun, Z. (2024, May). *Restraint design for obese occupants: Obese GHBMC model modifications* (Fourth of four parts. Report No. DOT HS 813 540d). National Highway Traffic Safety Administration.

Page intentionally left blank.

Technical Report Documentation Page

1. Report No. DOT HS 813 540b	2. Government Accession No.	3. Recipient's Catalog No.
4. Title and Subtitle Restraint of Design for Obese Occupants: Rear-seat Simulations (Second of four parts)		5. Report Date May 2024 6. Performing Organization Code
7. Authors Jason R. Kerrigan, Jason Forman, Bronek Gepner, Hamed Joodaki, Zhaonan Sun		8. Performing Organization Report No.
9. Performing Organization Name and Address University of Virginia Center of Applied Biomechanics 4040 Lewis and Clark Dr. Charlottesville, VA 22911		10. Work Unit No. (TRAIS) 11. Contract or Grant No. DTNH2215D00022
12. Sponsoring Agency Name and Address National Highway Traffic Safety Administration 1200 New Jersey Avenue SE Washington, DC 20590		13. Type of Report and Period Covered . 14. Sponsoring Agency Code
15. Supplementary Notes		

16. Abstract

This study evaluates the biofidelity of Global Human Body Modeling Consortium models representing obese people by comparing their kinematics with obese postmortem human surrogates in frontal sled tests. It was necessary to develop a finite element model to define accurate boundary conditions. Experimental tests with a robotic arm as well as an Instron machine were performed on the seat cushion and seat back foam to characterize the mechanical properties of the buck components. Then, the seat, seat back, frame, and seat reinforcement structure were 3D-scanned, cleaned, and meshed. Finally, the mechanical properties of the buck components were tuned based on the experimental tests. To investigate whether the model is capable of submarining, additional simulations (each with a modification to the model) were performed. The results showed that adding mass to the abdomen or removing the abdominal organs did not change the model's behavior significantly.

17. Key Words	18. Distribution Statement
GHBMC, obese, sled tests, Global Human Body Modeling Consortium	This document is available to the public from the DOT, BTS, National Transportation Library, Repository & Open Science Access Portal, https://rosap.ntl.bts.gov.

19. Security Classif. (of this report)	20. Security Classif. (of this page)	21. No. of Pages	22. Price
Unclassified	Unclassified	42	

Page intentionally left blank.

Table of Contents

List of Figures

List of Tables

Executive Summary

Task 1 of this study evaluates the biofidelity of obese Global Human Body Modeling Consortium (GHBMC) models by comparing their kinematics with obese postmortem human surrogates (PMHS) in frontal sled tests. The PMHS tests were performed previously at the University of Virginia Center for Applied Biomechanics (Joodaki et al., 2015). Briefly, two obese PMHS were the subjects for frontal sled tests at two different speeds (29 and 48 km/h) in the sled buck created from a rear seat of a sedan. The weight (124 kg) and body mass index (BMI) (35 kg/m^2) of one of the obese GHBMC models matched with those of an obese PMHS. This subject was chosen for the purposes of comparison.

Prior to the simulation of sled runs and to define accurate boundary conditions, it was necessary to develop a finite element model (FEM) of the buck. Experimental tests with a robotic arm as well as an Instron machine were performed on the seat cushion and seat back foam to characterize the mechanical properties of the buck components. Then, the seat, seat back, frame, and seat reinforcement structure were 3D scanned, cleaned, and meshed. Finally, the mechanical properties of the buck components were tuned based on the experimental tests.

Afterwards, the GHBMC model representing a 70-year-old person with the height of 188 cm and BMI of 35 kg/m^2 was positioned on the seat like the PMHS positioning. The buck model received the same acceleration as the physical sled test. The head, shoulder, pelvis, and knee trajectories as well as the torso angle time history of the obese model were compared with those of the obese PMHS.

The PMHS exhibited substantial forward motion of the lower body and subsequent backward rotation of the torso, affected by the limited engagement of the lap belt with the pelvis (submarining). This characteristic has proven challenging with regards to designing new safety tools for obese occupants. The obese model was unable to replicate this behavior. Most notably, the lap belt remained engaged with the boney structure of the pelvis throughout the simulation which prevented the model from submarining.

To investigate whether the model is capable of submarining, additional simulations (each with a modification to the model) were performed. First, the mass distribution of the model changed by adding mass to the abdomen and decreasing the mass of the arms. Adding mass to the abdomen was done in two different ways: (1) adding mass to the pelvis, and (2) adding mass to the abdominal organs. Second, all the abdominal organs of the model were removed to see if a model with a hollow abdomen could submarine. Third, using two simulations with more slouched positions aided to investigate the effect of torso angle on submarining. Fourth, a simulation with a slouched position and increased pelvis mass was performed to see if the combination of different effects can make the model submarine. Fifth, the material properties of the flesh were modified to see if a model with softer flesh can submarine.

The results showed that adding mass to the abdomen or removing the abdominal organs did not change the model's behavior significantly. In addition, although with a more slouched positioning the model's tendency to submarine increased, the lap belt remained engaged with the pelvis and the subject remained restrained by the seat belt. However, changing the material properties of the flesh proved to be promising. Finally, several of these findings were in a peer reviewed publication (Gepner et al., 2018)

Page intentionally left blank.

Summary of Findings

- Unlike the obese PMHS, the obese model did not submarine (submarining defined as the pelvis sliding under the belt as the belt applies load to the abdomen).
- It is speculated that the shear stiffness of the abdominal flesh permits the belt to slip.
- The shear deformation of the adipose tissue did not facilitate the seat belt to move upward and disengage the pelvis.
- Modifying the body mass distribution did not change the results substantially.
    - The model did not submarine with an increased pelvis mass.
    - The model did not submarine with an increased mass of abdominal organs.
- A model with a hollow abdomen did not submarine.
- With a more slouched position, the model's tendency to submarine increased. However, the lap belt remained engaged with the pelvis and the subject restrained by the seat belt.
- By increasing the pelvis mass of slouched model, the behavior of model did not change substantially.
- Decreasing the compression stiffness of the flesh material by a factor of 10, resulted in increased compression of adipose tissue under the lap belt load.
- Decreasing the compression stiffness of the flesh material increased the belt penetration into the abdomen. However, this model also did not submarine.
- Although the obese model did not submarine, it experienced a significant lower extremity forward motion, which was a result of
    - increased mass, and
    - delayed engagement of the pelvis due to the increased thickness of adipose tissue.
- It was speculated that by decreasing the coupling between the flesh and pelvis one could make the obese model submarine. However, such a modification might not be biofidelic.
- Since it is likely that belt/pelvis/abdomen interaction is responsible for at least some of the increased injury risk for obese occupants, biofidelic belt-to-pelvis interaction is paramount for the injury risk evaluation and countermeasure development.
- The improved models of abdominal flesh, and specifically subcutaneous adipose tissue, should be considered before using obese models to predict injury risks to obese occupants in crash simulations.

Page intentionally left blank.

UVA Rear Seat Characterization and Modeling

This task evaluates the biofidelity of obese GHBMC models by comparing their behavior in a frontal sled test with that of the PMHS. To do a valid evaluation, the boundary conditions should be defined correctly. In this effort, development of a FEM of the buck, with which the PMHS sled tests were done, was necessary. The ideal buck FEM should have, not only an identical geometry as the physical model, but also the same mechanical behavior. The following section details the process of mechanical properties characterization and FEM development of the rear seat buck.

Seat Mechanical Properties Characterization

The seat and seat back mechanical properties of the buck were characterized via different experiments using a 6-°-of-freedom robotic arm (KUKA Robot, KR300 R2500 Ultra) along with an Instron machine. The KUKA robot had a 6-°-of-freedom load cell attached to the end effector, which allows for both force and position control, with a 0.06 mm position accuracy and a 2.5 ms (400 Hz) control loop. Along with a 25,000 mm radius range of motion (ROM), and 3,500 N payload capacity, the robot was an ideal tool for desired component testing.

A data acquisition system (DAS) consisting of linear accelerometers and 6DX cube provided additional measurements in case of inertial effect compensation. Furthermore, a Romer arm was used to develop a unified coordinate system between the robot, DAS load cell, and seat. Figure 1 shows the test setup for mechanical properties characterization of the physical seat. A spherical indenter and the pelvis of a Hybrid III dummy were attached to the robot for calibration and validation tests, respectively (Figure 2).

Table 1 shows the test matrix of the seat mechanical properties characterization. Indentation tests at several rates at several locations were done on both the seat and seat back to capture the stiffness. Torsion tests and slide tests at several rates and with different normal forces measured the friction properties of the seat. Torsion tests were done with and without fabric used for PMHSs' clothing in the sled tests. For these tests the fabric was wrapped around the indenter and Hybrid III dummy pelvis.

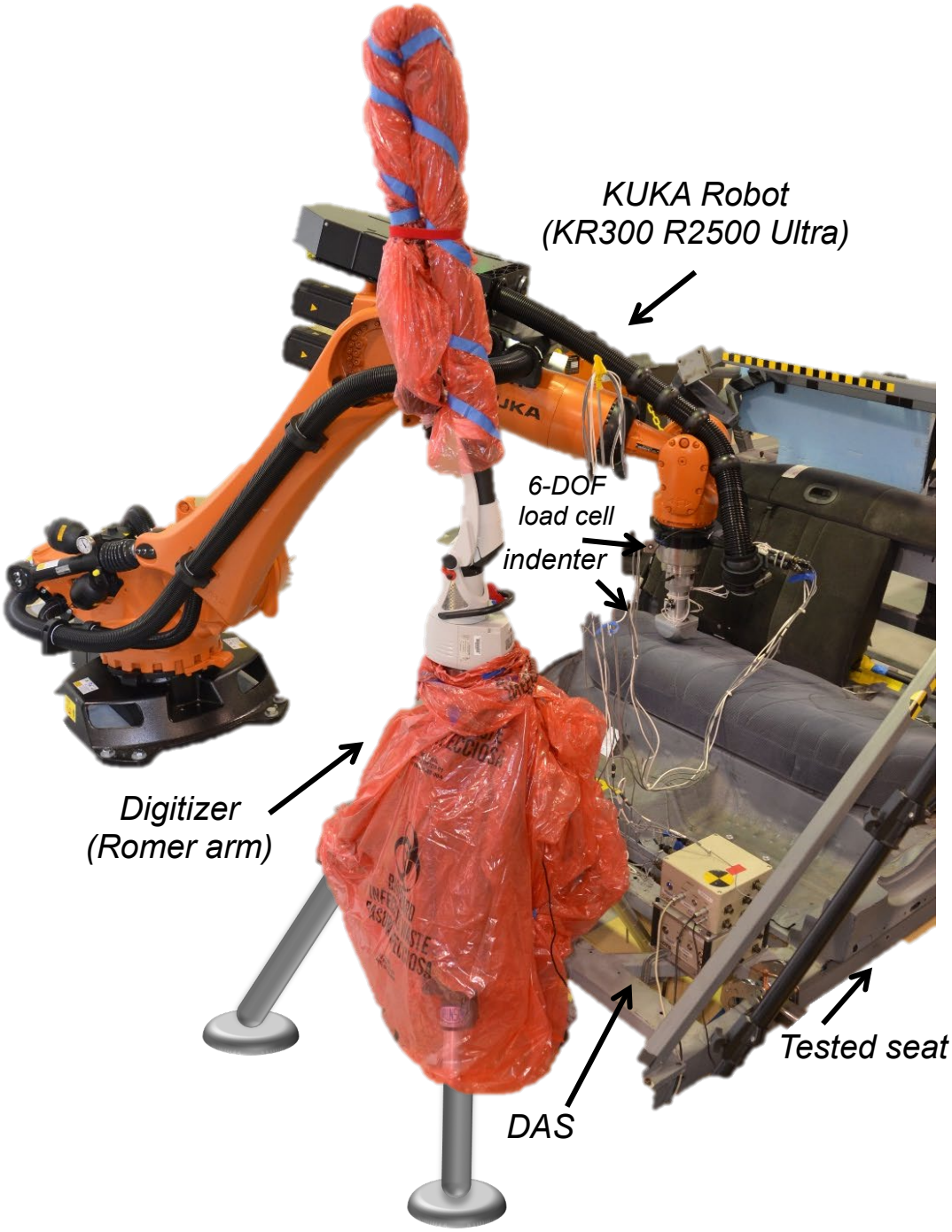

Figure 1. Seat mechanical properties characterization test setup

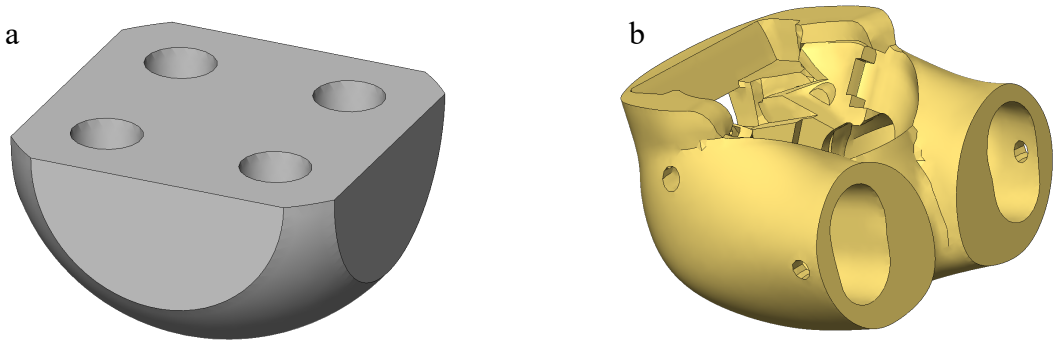

Figure 2. Schematic figure of the indenter (a), and Hybrid III pelvis (b) attached to the robot for calibration and validation test suit, respectively

Table 1. Test matrix of seat mechanical properties characterization

Component	Test
Calibration (With Indenter)	
Seat	Indentation Test (Several Rates/Locations)
	Torsion Test w/ and w/o cloth (Several Rates/Normal Forces)
	Slide Test (Several Rates/Normal Forces)
Seat Back	Indentation Test (Several Rates/Locations)
Validation (With Hybrid III Pelvis)	
Seat	Indentation Test (Several Rates/Locations)
	Torsion Test w/ and w/o cloth (Several Rates/Normal Forces)
	Slide Test (Several Rates/Normal Forces)

Not all the collected data was used for the development and validation of the rear-seat FEM. Some tests provided additional, redundant data; however, its use was not necessary during the model development. Only the data used for this task is included in the report.

Instron Testing

Foam specimens with the dimension of 65×70×72 mm (width×length×height) were cut from the seat cushion and subjected to compression test using an Instron machine (Figure 3). A triangular (ramp) displacement time history at a quasi-static rate (0.01 Hz for a complete cyclic triangular displacement time history) was applied to the foam to measure the stiffness of the material. Figure 4 shows the results of this test.

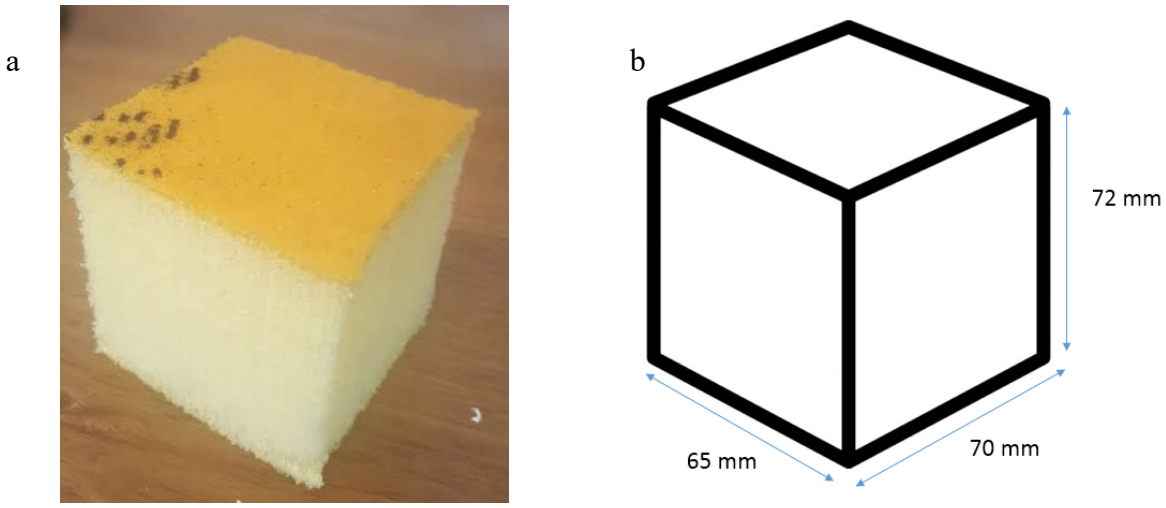

Figure 3. The foam specimen cut from the seat cushion (a) and its dimensions (b)

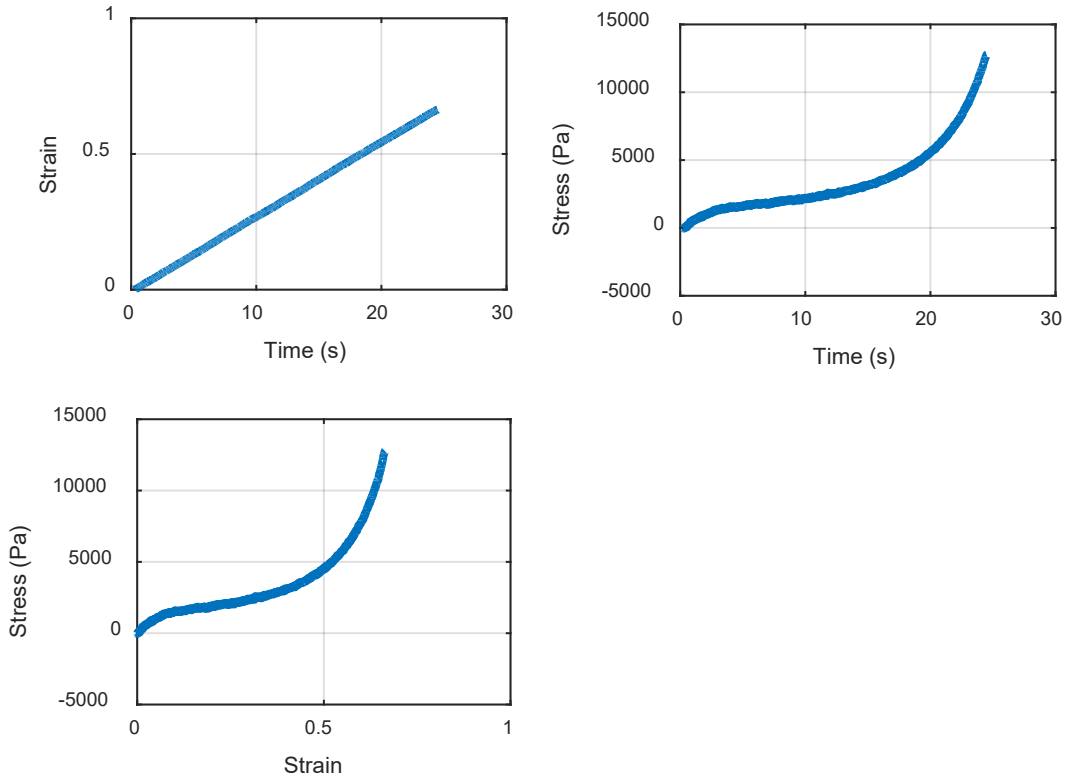

Figure 4. Results of compression test with Instron on the seat cushion foam sample

Finite Element Modeling of the Seat

Scanning the Buck

The scanning process was done using a 3D Romer arm. An SAE vehicle coordinate system, following the SAE J211 (Society of Automotive Engineers, 1995), was developed for the buck, with the x-axis being forward, y-axis from driver to passenger side, and z-axis (based on the right-hand rule) downward (Figure 5).

Figure 5. The global coordinate system

First, both seat and seat back were removed to scan the surface of the buck. Then the seat and seat back were installed again and scanned. Because the buck, seat, and seat back were symmetric, only the passenger side was scanned.

Additionally, several characteristic points of the buck were digitized. These included the following.

- outboard lap belt anchor bracket, (center of webbing)
- retractor belt slot, center
- retractor belt slot, right corner
- retractor belt slot, left corner
- buckle bolt, center of head
- H-point reference x position
- H-point reference z position
- Some points on the reinforcement structure of the seat cushion (to be used in modeling)

Cleaning the Scan and Meshing

After scanning the buck components, the scanned surface was cleaned in Geomagic Control software.[1] Then, surfaces were created from the cleaned scan in Geomagic Design X software. Since only half of the buck (passenger side) was scanned, the surfaces were reflected to complete the geometry.

[1] Design X, Control X, Wrap, and Geomagic for SOLIDWORKS software by Artec 3D, Senningerberg, Luxembourg; U.S. office in Santa Clara, CA.

Afterwards, the surfaces were imported to Hypermesh software for meshing. Buck steel structure was meshed using triangular shells, seat back was meshed via tetrahedral solids, and the seat cushion was meshed using hexahedron brick elements.

Next, the meshed components were imported to an LS-Prepost preprocessor to complete the model of the seat. The seat reinforcement structure geometry was developed using LS-Prepost and meshed using beam elements. BEAM_IN_SOLID keyword defined the interaction between the reinforcement structure and the seat foam cushion. Material properties for the steel and aluminum parts of the test setup was obtained from the literature and implemented in the model.

a

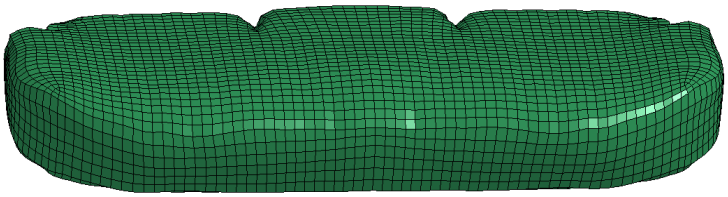

b

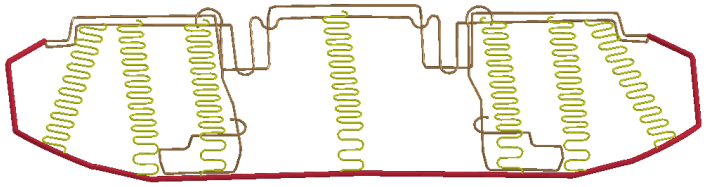

c

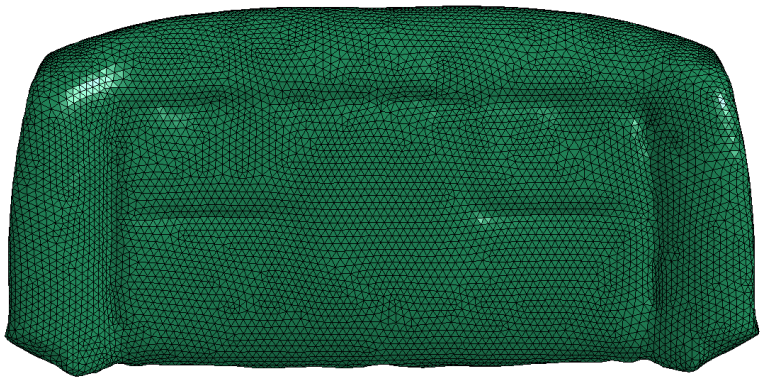

d

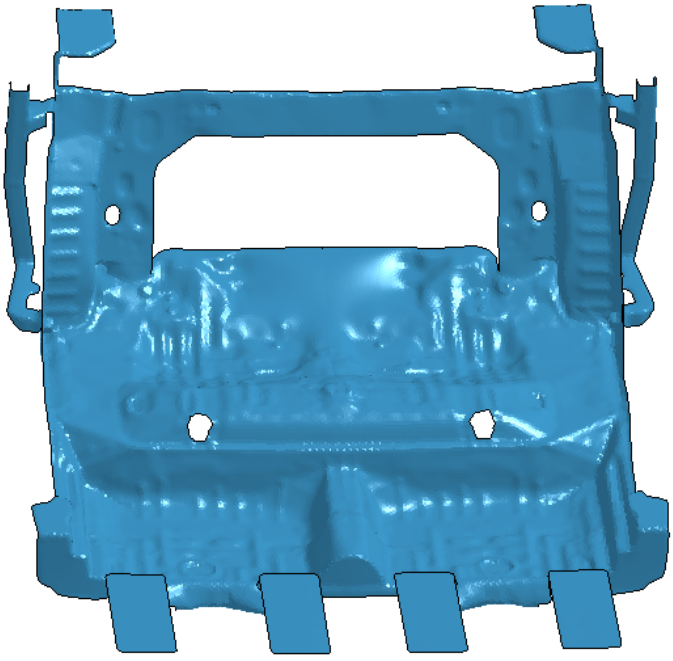

Figure 6. A meshed model of the seat (a), seat reinforcement structure (b), seat back (c), and frame (d). The mesh for reinforcement structure and frame are turned off for visualization considerations.

Optimizing the Material Properties Using Experimental Data

The cushion foam stress-strain curve obtained from an Instron compression test was directly implemented into the FEM as an input for the MAT_LOW_DENSITY_FOAM material model. No rate sensitivity parameter was used and hence, the cushion was modeled as a hyperelastic (non-linear elastic) material. To evaluate the seat stiffness, the robotic arm indentation tests (using an aluminum impactor) were simulated using the FEM. The results showed that with 250 N compression (z-direction) force, the normal displacement of the impactor in the finite element simulation is within 3 cm of that in the physical experiment. The difference in impactor displacement between the finite element simulation and the physical test was highest at the rear of the seat. This could be explained by a gap between the seat cushion and the frame observed in the physical model. Hence, the initial impactor displacement resulted in the rigid body motion of the seat until it came in contact with the frame. However, this effect was not modeled in the FEM of the seat. Consequently, since the occupant submarining was of paramount interest in this study, it was decided that the stiffness of the front of the seat is the most important and it matched well with the experimental and finite element results.

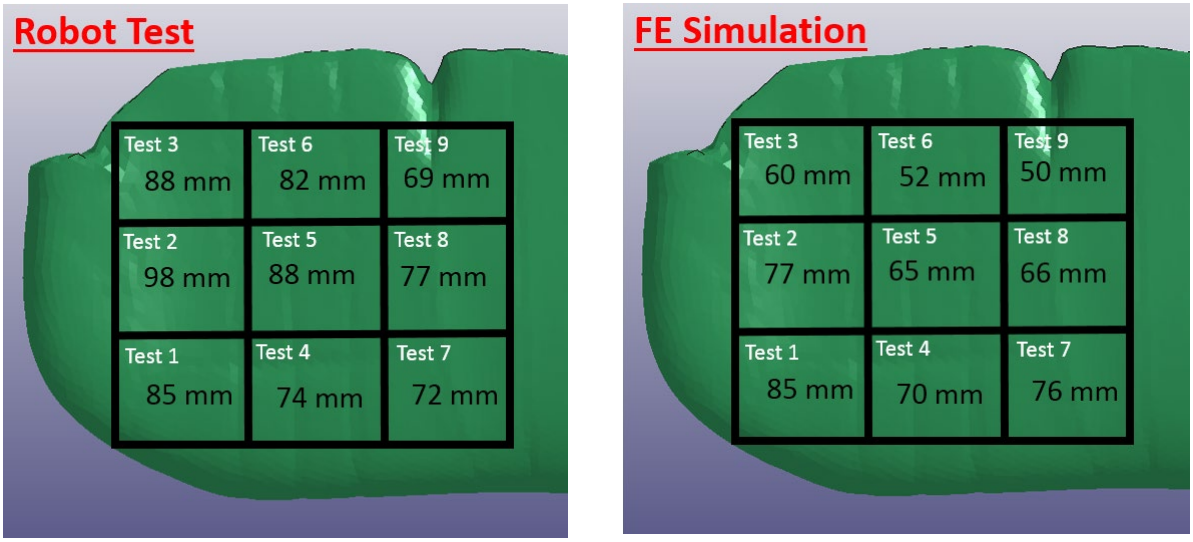

Figure 7. Impactor displacement (mm) at different locations with 250 N compression force. The results of the finite element simulation (right) and experiment (left).

The mass of whole physical seat (consisting of the cushion and the reinforcement structure) was measured directly. The volume of the seat and the mass of the reinforcement structure was estimated from the model. Given that information, the density of the foam was estimated to be 101 kg/m^3.

To find the optimum friction properties for the cushion-indenter interaction, the results of the quasi-static robotic arm slide test were used. In the physical test, a normal (z-direction) force followed by an x-displacement movement was applied to the indenter and the z-displacement and force in x-direction were measured. A similar condition was applied to the FEM. Different friction coefficients were implemented to the contact definition. Using a friction coefficient of 0.32 was found to produce acceptably similar results to that of the physical test.

Positioning the Obese GHBMC Model

It was found that the height and weight of one of the obese GHBMC models (BMI 35 kg/m^2, 188 cm, 70 years old) matched with PMHS 404 used in the University of Virginia sled tests (Joodaki et al., 2015). Hence, the selected GHBMC model was positioned to match the position recorded for the PMHS 404 in Test 1333 (Figure 8). The following steps were taken to achieve the desired position for simulation.

- Positioning the GHBMC model close to the seat
- Femur angle positioning
- Tibia angle positioning
- Settling
- H-point positioning
- Torso angle positioning
- Positioning feet on the toepan
- Positioning the arms
- Belt routing
- Sled run simulation

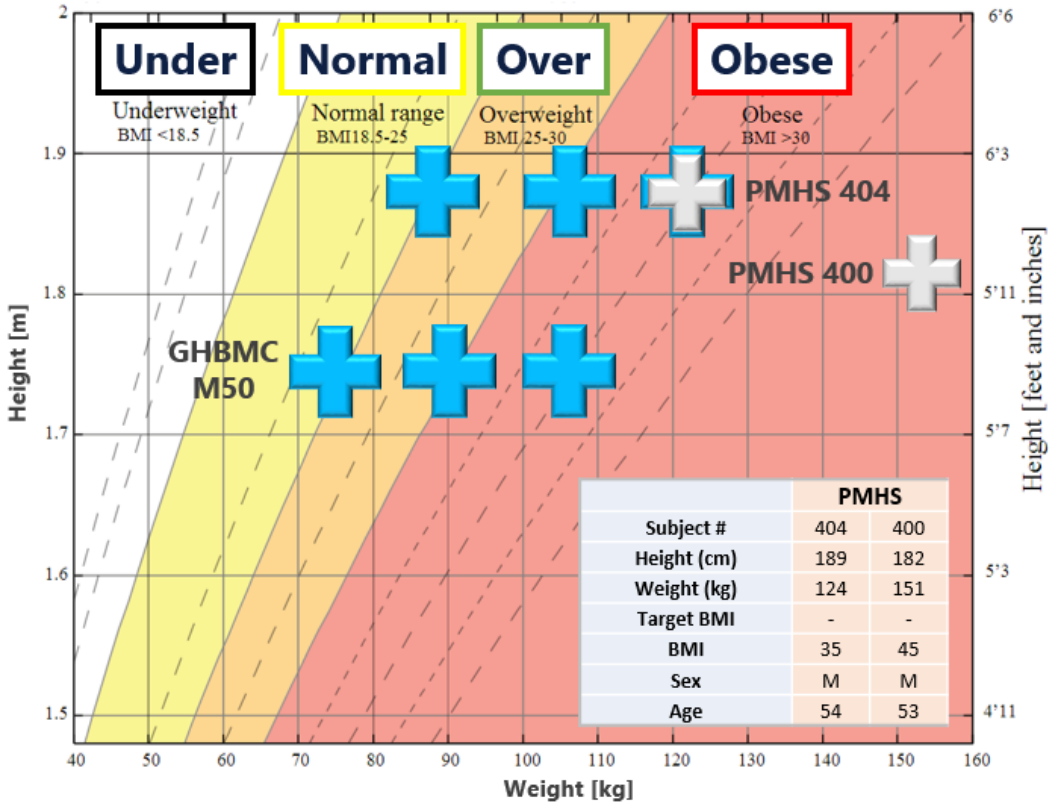

Figure 8. Height, weight, and BMI of available models (blue) and the two obese PMHS (gray). The different BMI ranges (underweight, normal, overweight, and obese) are illustrated with different colors.

Each of these steps is described below in detail. After each positioning step, the nodal coordinates were extracted from the simulation results and used as input for the next step. Additionally, a MATLAB code was used to modify the coordinates of the GHBMC nodes which are used for the joint definition to avoid any initialization errors for the next simulation.

Positioning the Model Close to the Seat

First, the model was moved as close as possible to the seat without penetration to the seat or seat back. This step was carried out through a rigid body motion, without running any simulation. Additionally, the GHBMC's model torso angle was set as close as possible to that of the target PMHS.

Femur Angle Positioning

Node numbers 9023210 (proximal point) and 8127934 (distal point) were used to position the right femur. First the projected angle of the line that these points make with a horizontal line in xz-plane was calculated (14°). Then knowing the target angle (23°), the target position of the node 8127934 was calculated (holding node 9023210 constant). Afterwards, a normalized vector was defined from the initial position of the node 8127934 to its target position with the magnitude of the vector given as the displacement scale factor in the model. This node was moved using the node prescribed motion keyword. A similar process was repeated for the left femur using the nodes 7047435 (proximal point) and 8127918 (distal point). The upper extremity bones were constrained in every translational and rotational direction during this process using SPC set keyword.

Tibia Angle Positioning

A procedure similarly used for measuring the knee angle was used for the tibia using the nodes 9011739 (proximal point) and 9001773 (distal point). The calculations showed that the model tibia angle (52°) is very close to the target angle (53°). Hence, no simulation was conducted for changing the tibia angle in this step.

Settling

Model settling was carried out through a separate simulation. To shorten the simulation time, a node set including all nodes of the GHBMC was defined and an initial velocity of 1 m/s was applied to that node set. This initial velocity along with gravity forced the GHBMC to settle down into the seat.

The lower extremity bones were constrained in all rotational directions to prevent any change in the femur and tibia angle (which were modified in the previous steps). A similar constraint was applied to the arm bones as they were to be positioned later. However, no constraint was applied to the other parts of the upper body.

H-point Positioning

Two reference points for measuring the H-point position (one for indicating the x position and one for z-position of the reference) were marked on the buck frame when positioning the obese PMHS. The position of the H-point with respect to that point was measured during PMHS tests. As mentioned before, the x and z coordinates of that reference point were digitized. Hence, positioning the obese model H-point could be performed accordingly.

Because of the implicit uncertainty in identifying the H-point in the PMHS tests (especially with the obese PMHS), the outermost points of the greater trochanters were identified and treated as the H-point. Consequently, the equivalent points on the obese GHBMC (nodes 7500194 and 9054246 on the left and right side of the model, respectively) were chosen and moved accordingly.

The spine and lower extremity bones were rotationally constrained. A prescribed displacement in x-direction was applied to those two nodes with a magnitude equal to the difference between the target and initial x-position. For this simulation, the friction between the GHBMC and the buck compartments was decreased to a very small number for the model to move smoothly.

Torso Angle Positioning

The initial torso angle (the torso angle after step 5, 71°) was measured using the outermost node on the femurs (nodes 7500194 and 9054246 on the left and right side, respectively) and nodes on the acromion (nodes 4001033 and 4148645 on the left and right side, respectively). To match the PMHS torso angle (69°) the target positions of nodes on the acromions were calculated using an approach like femur angle positioning (step 2). The lower extremity bones (including the pelvis) were constrained in all rotational and translational directions. Additionally, the arms and skull were rotationally constrained.

Positioning Feet on Toepan

Although the femur and torso angle of the model were set to replicate those recorded in the case of the PMHS, the obese model feet ended up penetrating the toepan. The reason for that was the difference between the lower extremity length of the PMHS and the model (despite having similar stature). Consequently, the lower extremities (femur and tibia angle) were adjusted to fit the occupant into the model of the buck.

Positioning the Arms

As the next step, the arms were positioned by placing the hands on the femurs. To do so, the position of a node on the left ulna (node 3009700) and a node on the outer surface of the left thigh (node 7514661) were determined. Then the direction and magnitude of the vector from the node on the ulna (tail of the vector) to the node on the thigh (head of the vector) were calculated. This vector was defined and used to define a prescribed motion for the node on the left ulna. Since the model was symmetric, a mirrored vector (opposite y-direction), was assigned to a node on the right ulna (node 7514661).

Belt Routing

The model of a retractor used in the PMHS sled tests with pre-tensioner and force limiter was obtained from Autoliv. The belt webbing was created in house using the options available in LS-Prepost preprocessor. First, using keyword SetD, two sets of segments were created by choosing the shells that the shoulder and lap belt should be wrapped around. Then, using BeltFit keyword, mixed seat belt elements were created to represent the shoulder and lap belt (Figure 9(a)). The seat belt elements which had penetrated to the flesh were moved using the Translt option. Also, the shapes of some elements were corrected using the ElEdit option.

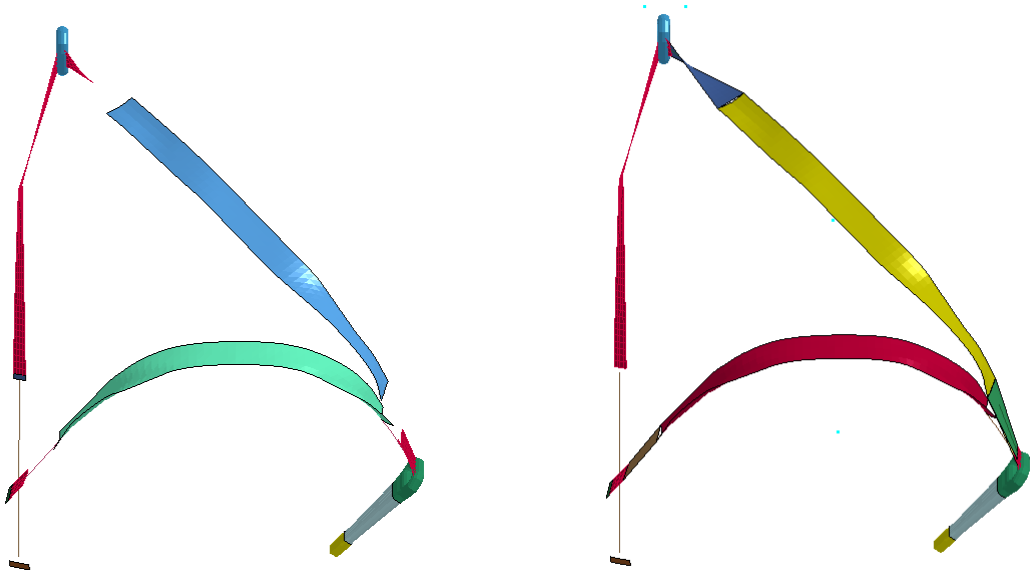

(a) (b)

Figure 9. (a) Seat belt elements created to represent the shoulder and lap belt (b) Connecting new seat belt elements to other seat belt parts

To connect the pieces of seat belt together, those parts of the created seat belt elements that were not attached to the body were removed and then, a new mesh between the created seat belt elements and the D-ring, seat belt tongue model and end bracket elements were cast using BMesh option (Figure 9(b)). All the pieces of the seat belt were attached together by the Replace Node tool in the ElEdit option (Figure 10). Next, all the created parts were merged into a single part.

Prior to node replacement After node replacement

Figure 10. Attaching seat belt pieces

The seat belt was modeled using the new 4-point shell seat belt formulation, and since the current version of LS-Prepost did not provide a support for these types of elements, these keywords needed to be modified manually, working directly with the text file. To achieve this all the nodes and elements of the seat belt were outputted into a key file using the Output keyword. The key file of the seat belt model then was opened in Notepad++ software to be modified. The seat belt elements were changed to shell elements. To do so, sbrid and slen columns had to be deleted. The file was saved and reopened in the LS-prepost. Then, all the segments were defined with the new elements and nodes. Again, Notepad++ was used to retrieve the format for 4-point

seat belt elements, suitable for LS-Dyna solver. Figure 11 shows the positioned 35 kg/m^2 BMI obese GHBMC in two different views.

(a) (b)

Figure 11. Positioned 35kg/m^2 BMI obese GHBMC: (a)ZX plane (b)YZ plane

Sled Run Simulation

Finally, a sled test simulation was performed. An acceleration pulse from the University of Virginia 1333 test (Joodaki et al., 2015) (48 km/h, Figure 12) was used as an input. The head, shoulder, pelvis, and knee trajectory of the model were compared with those of the PMHS.

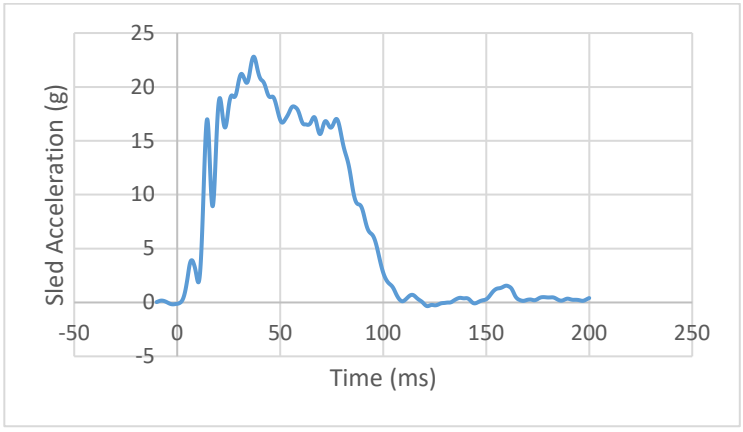

Figure 12. Sled acceleration of cadaveric test No 1333 used for computational simulation

Figure 13 shows the trajectory of different body segments of the obese model and PMHS. The lines connecting the head to the shoulder, and the shoulder to the pelvis are illustrated at four different time points: t= 29 ms, t= 58 ms, t= 87 ms, and t= 117 ms.

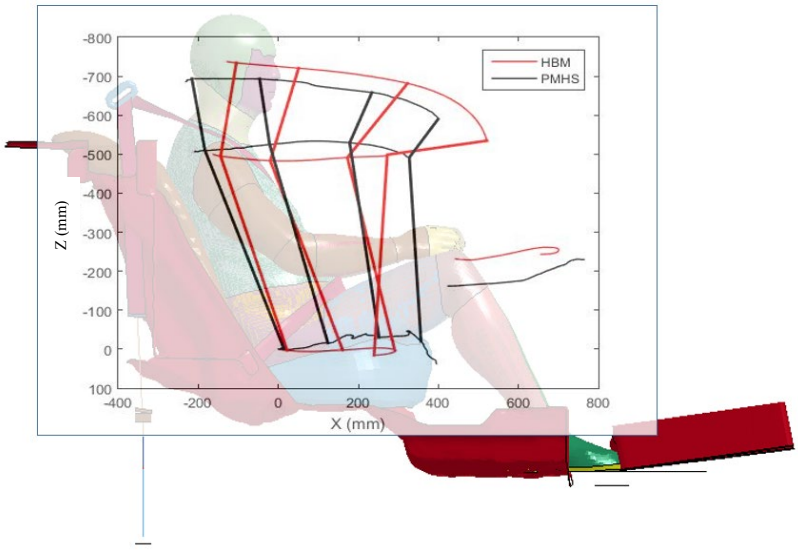

Figure 13. Comparison of the trajectory of the obese model and PMHS

The results showed that contrary to the obese PMHS, the obese model did not submarine. In the PMHS test, the lap belt did not engage with the boney structure of the pelvis. This resulted in a belt sliding above the pelvis and into the abdomen of the PMHS. Consequently, the subject exhibited an undesirable kinematics during the sled run, with the upper torso never pitching forward throughout the run. However, with the obese model, the lap belt z-position remained in the range of the pelvis z-position (in the global coordinate system, Figure 5) and hence, it applied force to the pelvis during the whole sled run. In addition, while the torso angle of the obese PMHS remained less than 90°, the torso of the obese model pitched forward towards the end of the run.

Analysis of Other Effects

As mentioned before, after running the rear seat sled test simulation, it was observed that the model's response was not like the PMHS. Because the highlighted differences were identified to be some of the most challenging for the development of an effective restraint system it was decided to investigate the nature of these differences. For this purpose, the following additional simulations were performed.

- Simulation with corrected head, torso, and femur angle
- Simulation with added mass to the abdomen
  - Added mass to the pelvis
  - Added mass to the abdominal organs
- Simulation with hollow abdomen
- Simulation with a more slouched position
  - Moving pelvis 5 cm forward
  - Moving pelvis 10 cm forward
- Simulation with combination of several effects

Simulation With Corrected Head, Torso, and Femur Angle

Comparing the trajectory of the PMHS and the human body model after the first simulation attempt, it was observed that the model's torso angle was slightly different from that of the PMHS obtained from the video trajectory. The reason for that was the fact that the torso angle was set based on the pre-test PMHS measurements, and these measurements were slightly different than the angles calculated from the reconstructed video trajectories. Additionally, as mentioned above, the model's knee angle was not like the one recorded for the PMHS due to differences in subject anthropometry. Both, torso and knee angles were adjusted in subsequent simulations in order to match the occupant positioning more closely. Finally, the head angle, which differed between the PMHS and FEM, was corrected to match the experimental initial conditions.

To match the model's torso angle with the PMHS torso angle calculated from the video trajectories, the shoulders were pushed back. This was done by defining the target location for the desired torso angle, and then defining a vector accordingly and assigning it (prescribed motion) to two nodes on the acromion. The skull, spine, and feet were rotationally constrained in x and z-directions. The arms and tibia were rotationally constrained in all three directions. The pelvis and femur were constrained in all 6° of freedom.

To modify the head angle, the head was first rotated around the y-axis until the model's Frankfurt plane was aligned with the global xy plane. Next the head was pushed back in the –x direction. During the head positioning, the head and spine rotation around the x and z axes was constrained. To ensure that the head does not rotate during the translation, a prescribed motion was applied to four different nodes, effectively constraining the rotation. During the whole procedure, the pelvis, arms, and legs were constrained in all 6° of freedom.

Next, the tibia angle was adjusted to match the PHMS measurements. The tibia was moved in –x direction, while constraining the femur (which already was at the correct angle) in all directions. Since it was impossible to fit the occupant FEM into the original model of the buck, the toepan model had to be adjusted. The toepan was extended in the z-direction to fit underneath the occupant's feet (Figure 14).

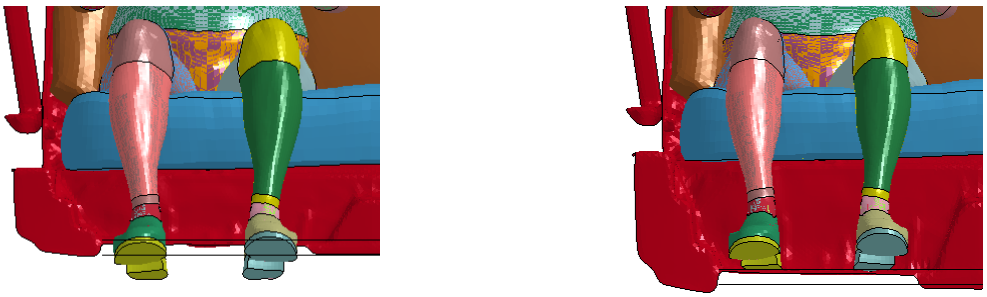

(a) (b)

Figure 14. Toepan extension: (a) Before extension (b) after extension

Afterward, the arms were positioned and the seat belt was routed similar to the method described above. When the positioning was completed, the sled run simulation was performed and the results were analyzed.

Figure 15 shows the trajectory of the obese PMHS and obese model with two different initial positions. The blue trajectory shows the results of the simulation with the "original" positioning described in the previous section, while the red trajectory illustrates the model behavior after making the positioning adjustments to match the video trajectory analysis obtained from the PMHS. The lines connecting the head to the shoulder, and the shoulder to the pelvis, are illustrated at four different time points: t = 7 ms, t = 58 ms, t = 87 ms, and t = 117 ms. Figure 16 compares the torso angle time history of the obese PMHS with that of the model with two different initial positions. The results illustrate that the model also did not submarine with the corrected position. Instead, the model pitched forward and experienced a torso angle of greater than 90°. While the initial torso angles were different for both "original" and "adjusted" positions, they became similar at around t = 80 ms (Figure 16).

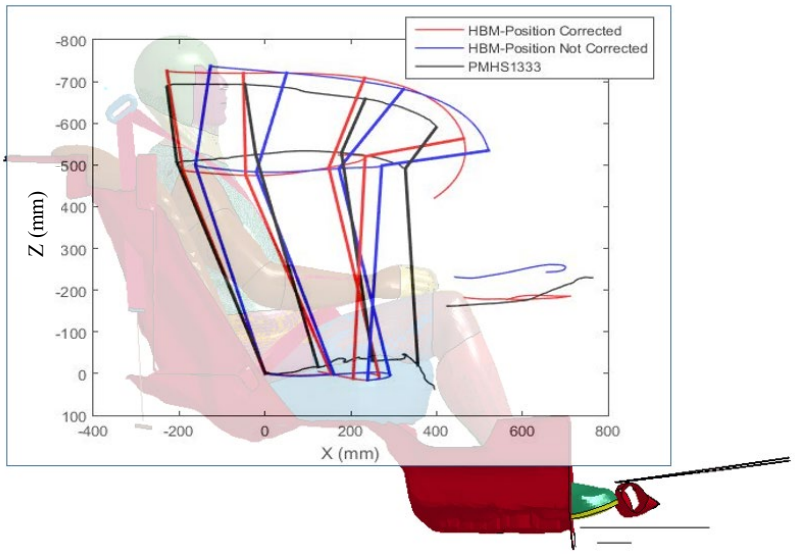

Figure 15. Trajectory comparison of the obese model simulation with two different initial positions and an obese PMHS

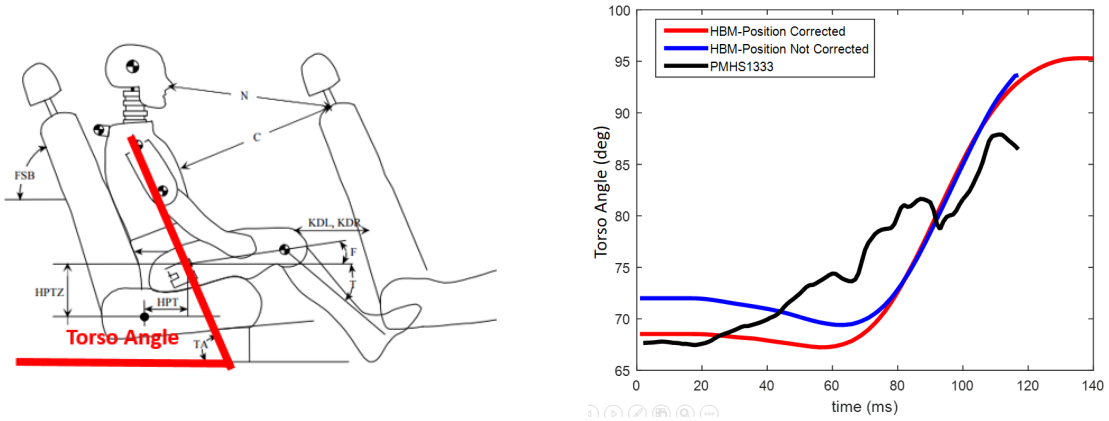

(a) (b)

Figure 16. (a) Definition of torso angle (b) comparison of torso angle between the obese PMHS and obese model with two different initial positions

Simulation With Added Mass to the Abdomen

During the review of performed simulations the question of appropriate mass distribution in the model was raised. It was speculated as to whether the abdominal mass distribution within the obese model could influence submarining behavior. One hypothesis was that the PMHS internal organs might have sag and fill the abdominal cavity, distributing more mass lower near the pelvis of the occupant. Two modifications were considered to evaluate this question: adding mass to the pelvis and adding mass to the abdominal organs. Below is a brief description of each modification.

Increased Mass of Pelvis

As the first option, the mass of the abdomen was increased by adding mass to the pelvis. The mass of the pelvis was increased by increasing the density of the ilium. While the initial mass of the pelvis ilium before modification was 0.6 kg, the mass was increased to 3.3 kg (2.7 kg mass added) by increasing the density with a factor of 5.5. To maintain the overall mass of the obese model, the density of the flesh and bones of the arms and hands were decreased. Then, the sled run simulation was performed. The simulation failed to run to completion due to a failure of a knee ligament element.

Another simulation with a 15 times denser pelvis ilium (mass: 9.04) was performed as well. Similarly, the mass compensation for this simulation was done by decreasing the density of flesh and bones of the arms and hands. Both simulations were performed with the “adjusted” occupant position.

Figure 17 illustrates the trajectory and torso angle time history of the model with no modification, the model with a 5 times denser pelvis ilium, the model with 15 times denser pelvis ilium, and PMHS. The results showed that increasing the mass of the pelvis does not change the behavior of model substantially. The models did not show the submarining behavior prior to the termination of simulation.

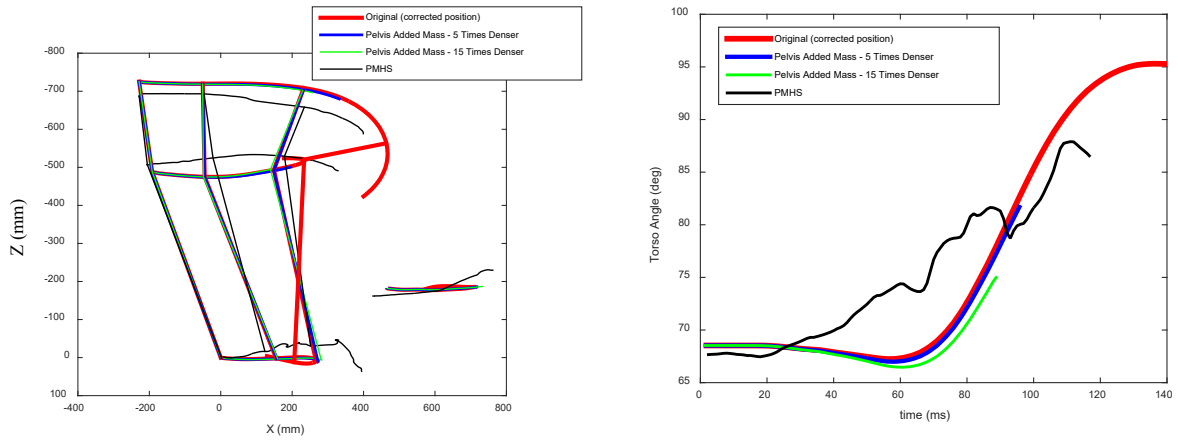

(a) (b)

Figure 17. Comparison of trajectory (a) and torso angle time history (b) of the model with no modification (red), the model with 5 times denser pelvis ilium (blue), the model with 15 times denser pelvis ilium (green), and the PMHS (black)

Increased Mass of Abdominal Organs

In another simulation, the mass of the abdomen was increased by adding mass to the abdominal organs. The parts that were modified were the colon, small bowel cavity, and duodenum (Figure 18). Initially, the overall mass of these parts was 1.86 kg. The mass after density modification was 4.63 kg (2.7 kg mass added). The sled run simulation was performed with the modified model. The simulation failed to complete due to an out-of-range force on some pelvis flesh nodes.

Figure 19 shows the trajectories and torso angle time histories of the sled run with the model without any modification, the model with added mass to the abdominal organs, and the PMHS. The results showed that adding mass to the abdominal organs would not change the model behavior substantially. The model did not submarine and pitched forward (torso angle greater than 90°).

Figure 18. Modified parts to add mass to the abdomen

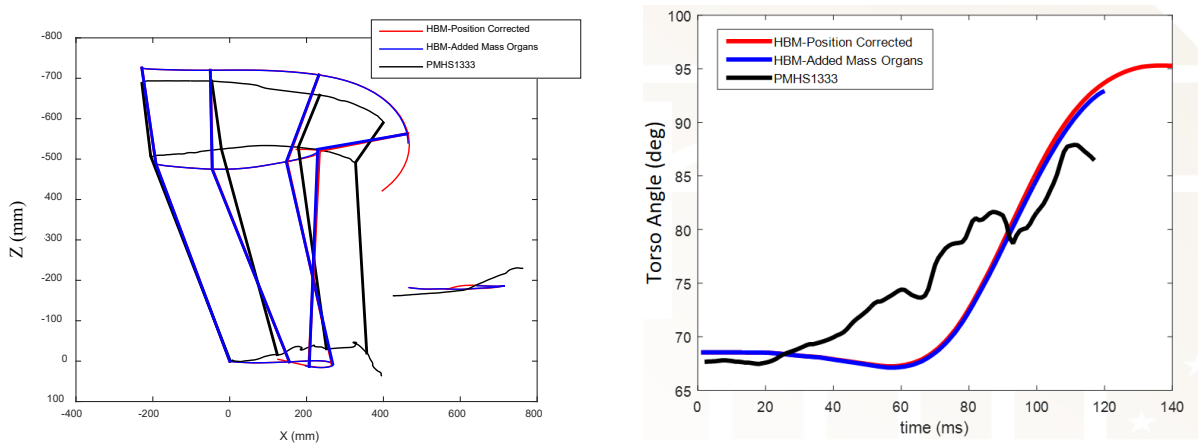

(a) (b)

Figure 19. Trajectories (a) and torso angle time histories (b) of the model without modification (red), model with added mass to abdominal organs (blue) and the PMHS (black)

Simulation With Hollow Abdomen

Another hypothesis to investigate was whether due to a GHBMC abdominal organ modeling limitation, the organs provide back pressure and a reaction force of additional support to the adipose tissue which prevents the belt from penetrating into the abdomen and the model from submarining. Hence, an extreme version of the GHBMC, where all the abdominal organs were removed from the model, was used to run the simulation. To do so, the abdominal organ elements were removed from the model. In addition, they were removed from the contacts in which they were included. This modification made the model unstable, which resulted in early termination of the simulation.

Figure 20 shows the trajectories and torso angle time histories of the simulation with the model without any modifications, the model with the hollow abdomen, and the PMHS. The change did not seem to have a substantial effect on the results prior to the termination of the simulation.

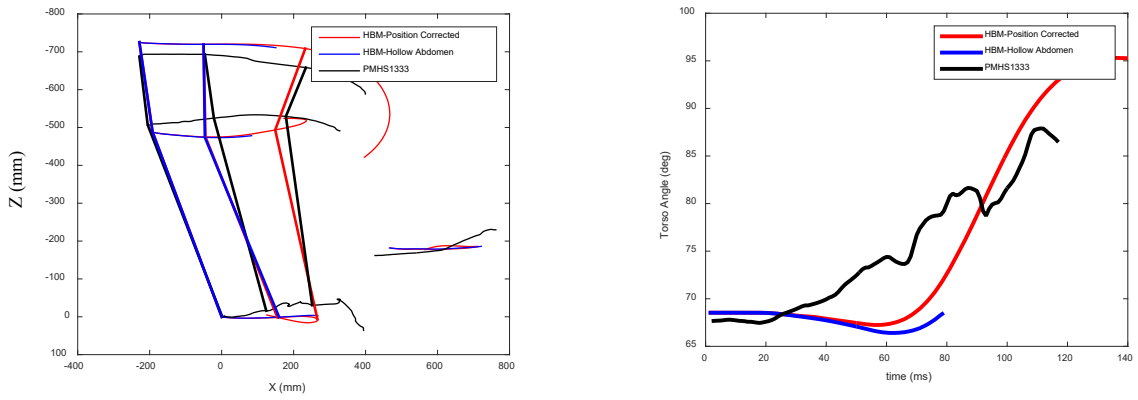

(a) (b)

Figure 20. Trajectories (a) and torso angle time histories (b) of the model with no modification (red), model with hollow abdomen (blue) and PMHS (black)

Simulation With a More Slouched Position

These simulations were aimed to investigate whether a more reclined position will result in the model pelvis submarining underneath the lap belt. To do so, two simulations were conducted with a modified occupant initial position. These included positions with adjusted pelvis location by moving it forward by 5 cm and 10 cm. For each simulation, first the pelvis was moved forward by applying a prescribed motion in the x-direction. During this step, the arms, hands, and head were constrained in all translational° of freedom, the femur and tibia were constrained in all rotational° of freedom, the spine and feet were prevented to rotate around x and z-direction, the pelvis was prevented to translate in y-direction, and the clavicles were translationally constrained in all directions.

Second, the arms were positioned via the method described earlier. Third, the tibia was pushed back while maintaining the femur angle. For the simulation with 10 cm forward motion, it was necessary to scale the toepan again. Finally, the sled run simulations were conducted with the new positions. The simulations failed to run to completion because of an out-of-range force on neck flesh nodes.

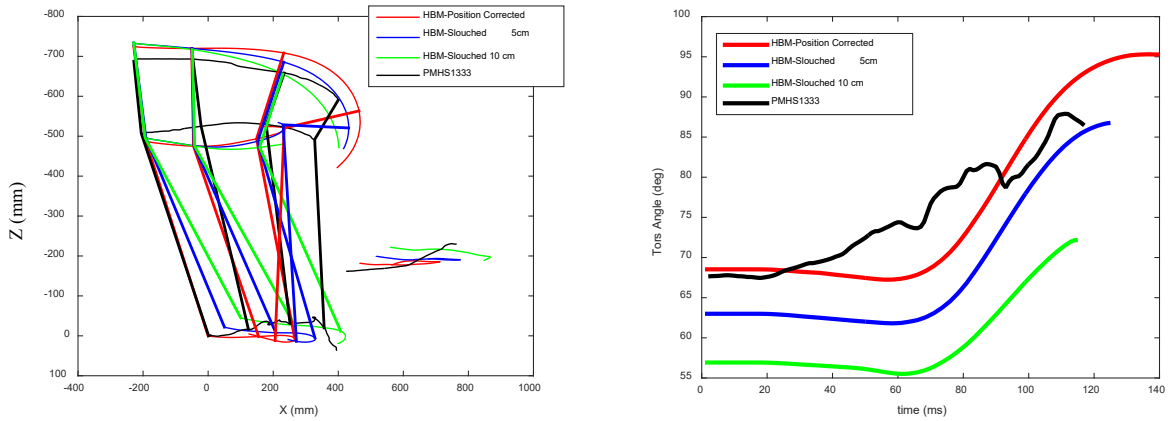

(a) (b)

Figure 21. The trajectories (a) and torso angle time histories (b) of the PMHS (black), the model with a position like the PMHS (red), and the models with pelvis 5 cm (blue) and 10 cm (green) more forward than the original position

Figure 21 shows the trajectories and torso angle time histories of the PMHS, the model with the original position, and the models with slouched positioning. The model with 10 cm forward pelvis position was on the verge of slipping off the seat edge (like the behavior that PMHS exhibited), however, in the end it was restrained by the lap belt. Moreover, although the lap belt almost reached the top of the iliac crest, it did not pass it and hence, the model did not submarine. The torso angle in both simulations with slouched positioning remained under 90°. However, this was due to the highly reclined (low torso angle) initial position. The rate of change of torso angle did not vary substantially between the simulations with the original position and the slouched positions (Figure 21).

Simulation With Combination of Several Effects

To investigate whether the combination of some of the aforementioned modifications makes a substantial change in model performance, a simulation with a slouched position (pelvis 10 cm forward) and added mass to the pelvis (5.5 times denser pelvis ilium) was performed.

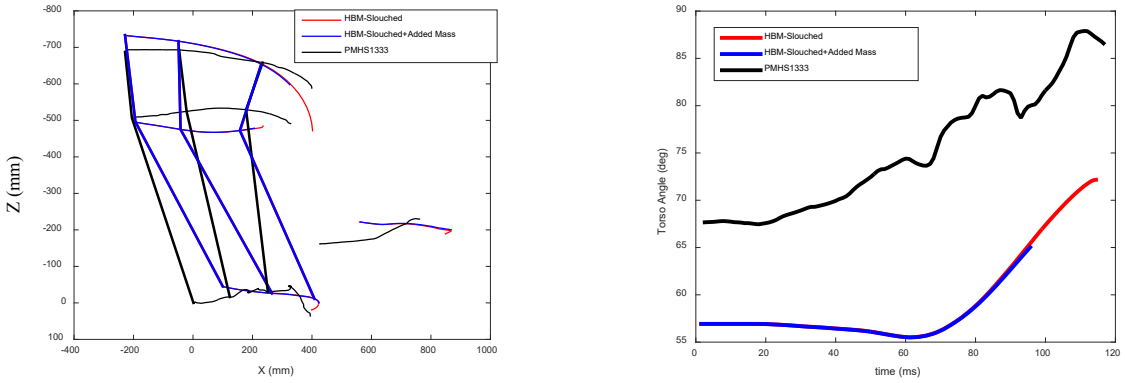

(a) (b)

Figure 22. Trajectories (a) and torso angle time histories (b) of the sled run with the PMHS (black), the slouched model (10 cm forward pelvis, red), and the slouched model with added mass to the pelvis (blue)

The results showed that adding mass to the pelvis does not change the model behavior with the slouched positioning (Figure 22). This conclusion was consistent with the results of the simulation with added mass to the pelvis with the original position.

Simulation With a Reduced Flesh Stiffness

Finally, a simulation with a slouched position (pelvis 10 cm forward) and reduced flesh stiffness was performed. The flesh material model was modified by changing the scale factor of the material stiffness curve (sfo of curve 1990002) from 1 to 0.1.

Figure 23 shows the trajectories and torso angle time histories of the PMHS and the slouched model with and without flesh material modification. The results showed that the tendency of the obese model to slip off the edge of the seat increased. This modification also decreased the torso angle throughout the simulation. However, the subject was again captured by the restraint system.

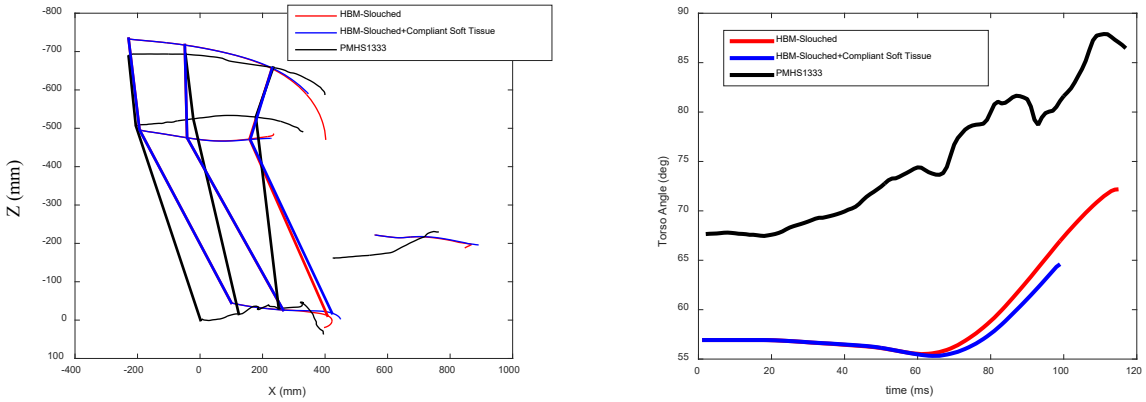

(a) (b)

Figure 23. Trajectories (a) and torso angle time histories (b) of the PMHS (black) and slouched model with original flesh material properties (red) and 10 times less stiff flesh (blue)

To evaluate the difference between the deformation of the abdominal soft tissues with the original and modified flesh mechanical properties, the relative distance between the node on the lap belt and a node on the pelvis was compared. Figure 24 illustrates that while the deformation of the abdominal soft tissue between the models with original position, slouched position, and hollow abdomen was almost similar, the model with a softer flesh experienced roughly 25 percent more deformation.

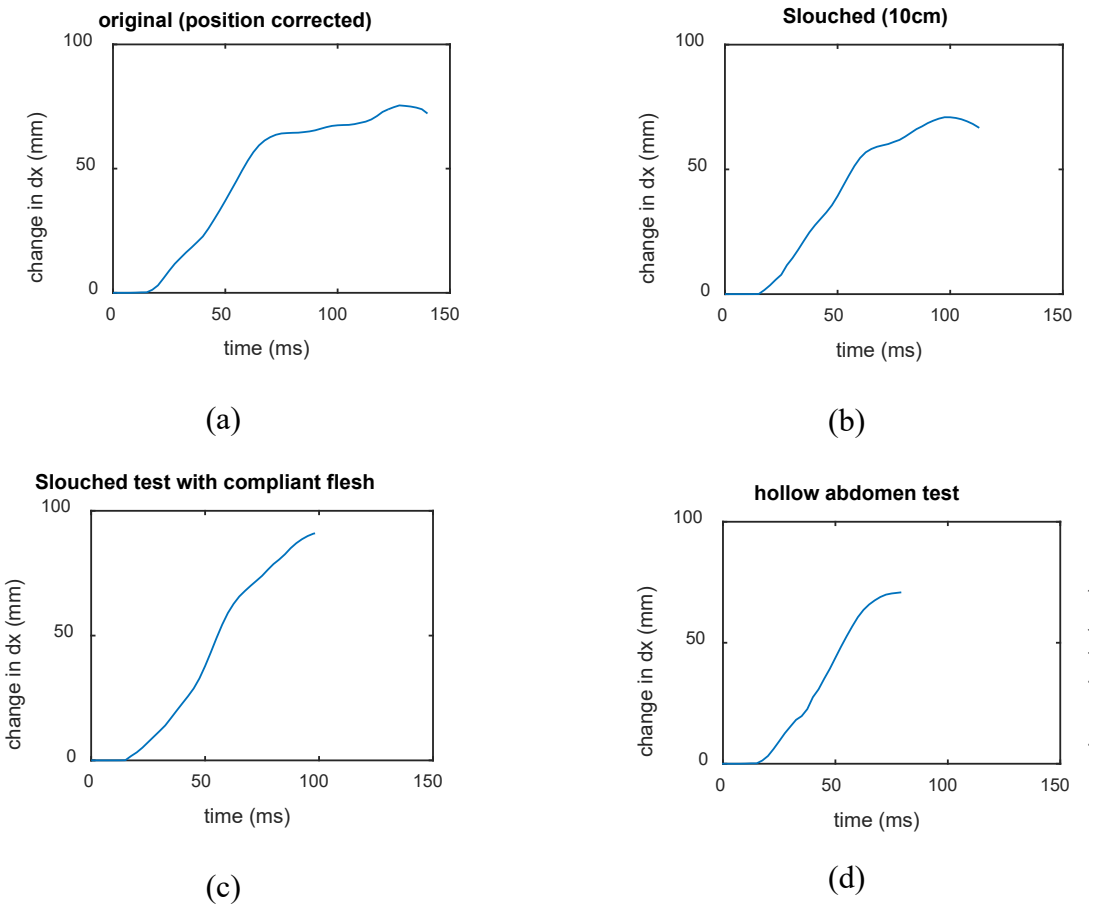

Figure 24. Change of difference in the x position (dx) of a node on the pelvis and a node on lap belt during four different simulations: (a) simulation with original position and original flesh material, (b) simulation with slouched model (pelvis 10 cm forward), (c) simulation with slouched model (pelvis 10 cm forward) and modified flesh material, and (d) simulation with original position, original flesh material, and hollow abdomen

Page intentionally left blank.

Conclusion

An FEM of the buck used in the UVA rear seat sled test series was developed. An obese model, which had the same BMI (35 kg/m^2) and height (188 cm) as one of the obese PMHS (PMHS 404) used in UVA rear seat sled tests, was chosen to evaluate the biofidelity of the models. More specifically, it was aimed at evaluating whether the obese model can facilitate submarining which was observed in case of the PMHS. Submarining was defined as the lap belt motion over the iliac crest of the pelvis without engaging, or after disengaging, the pelvis. In addition, submarining results in large lower extremity excursion, undesired torso angle (not pitched forward and ready for airbag deployment), and a greater likelihood of injury of the abdominal organs caused by the lap belt abdominal penetration.

The model was positioned following the CMM measurements from the PMHS test. The sled acceleration pulse was prescribed using the measured buck acceleration in test 1333 (Joodaki et al., 2015). The model failed to exhibit the same behavior that was observed in the case of the PMHS, and this was identified as a challenge in designing an effective restraint system for obese occupants. The lap belt remained engaged with the pelvis throughout the simulations and the model did not submarine. Furthermore, the torso pitched forward (torso angle greater than 90°) and was captured by the restraint system. This was contrary to the observations made during the PMHS test, where the occupant torso angle remained below 90°, and the occupant submarined and slipped off the seat.

To investigate the sensitivity of the model to different parameters and the ability of the model to predict occupant submarining, additional simulations with various modifications were conducted. The mass of the abdomen was increased, once by increasing the mass of pelvis and second by adding mass to the abdominal organs. The effect of the initial torso angle was also investigated by running two simulations with two different slouched positions (the pelvis moved 5 cm and 10 cm forward). Next, a simulation with a hollow abdomen was performed (abdominal organs were removed from the obese model). Additionally, a simulation with a slouched position (pelvis 10 cm forward) and added mass to the pelvis was performed to investigate the effect of the combination of different changes. Finally, a simulation with a slouched position (pelvis 10 cm forward) and 10 times less stiff flesh material was performed.

The results showed that adding mass to the abdomen does not change the model behavior substantially. The simulations with added mass resulted in similar trajectories and torso angle time histories from the original simulation. The model with the hollow abdomen was very unstable and hence, the simulation with that model terminated prematurely. The model did not show a substantially different behavior than the original model prior to the termination of the simulation. With the slouched position, the model showed a higher tendency to submarine and to slip of the seat, but it still did not submarine. Like the PMHS, the torso angle remained lower than 90°. However, this could be because the model had a lower initial torso angle. The rate of change of torso angle between the original and slouched positions was similar. The simulation with the slouched position (pelvis 10 cm forward) and added mass to the pelvis resulted in a similar trajectory and torso angle time history as the simulation with the slouched position and original pelvis mass. Finally, in the simulation with the slouched positioning (10 cm forward pelvis) and modified (10 times less stiff) flesh material, the model's tendency to submarine was the highest of all simulations. Modification of flesh material resulted in an increased pelvis excursion and decreased torso angle. Nevertheless, the model remained restrained by the restraint system and did not slip off the edge of the seat.

As the model was unable to replicate the characteristics that identified as a challenge in designing an effective seat belt for the obese occupants, using it for optimization of a rear seat restraint systems for this population is questionable. This applies in situations where no knee support (e.g., knee bolster) is available and the occupant relies solely on the lap belt engagement. Consequently, some modifications should be made to the model prior to the restraint system optimization task. These modifications could include the change in material properties of the flesh. More specifically, a constitutive model with lower shear stiffness might result in more accurate representation of PMHS kinematics (i.e., submarining). For this purpose, using an anisotropic constitutive model to specify the compression and shear stiffness separately can be useful. Additionally, decreasing the coupling of the pelvis and the flesh by modifying the contact between them is another promising option to investigate.

References

Gepner B., Joodaki H., Sun Z., Jayathirtha M., Kim T., Forman J., & Kerrigan J. (2018) *Performance of the obese GHBMC models in the sled and belt pull test conditions*. Proceedings of the IRCOBI Conference 2018, 12-14 September. https://www.ircobi.org/wordpress/downloads/irc18/pdf-files/60.pdf

Joodaki, H., Forman, J., Forghani, A., Overby, B., Kent, R., Crandall, J., Beahlen, B., Beebe, M., & Bostrom, O. (2015). *Comparison of kinematic behaviour of a first generation obese dummy and obese PMHS in frontal sled tests*. Proceedings of the IRCOBI Conference 2015, 9–11. https://www.ircobi.org/wordpress/downloads/irc15/pdf_files/57.pdf

Society of Automotive Engineers. (1995, March 1). *SAE J211/1 MAR95 instrumentation for impact test*. [Note: In 2006 the organization changed its name to SAE International.]

DOT HS 813 540b
May 2024

U.S. Department
of Transportation

**National Highway
Traffic Safety
Administration**

16164b-050324-v3